On the Interaction between Thin Isolated Eddies and Longshore Currents

DORON NOF

Department of Oceanography, The Florida State University, Tallahassee, FL 32306

(Manuscript received 2 October 1982, in final form 29 July 1983)

ABSTRACT

A simplified two-layer analytical model describing the interaction between a longshore current and a thin lenslike eddy is considered. The eddy is situated near a vertical wall and is embedded in a frictional boundary current which is flowing from one latitude to another. Attention is focused on the conditions under which the boundary current compensates for the tendency of the eddy to drift due to β so that the eddy is stationary. The model incorporates movements resulting from the circulation within the eddy, the longshore flow and β. Both the upper and lower layer are taken to be active; diffusion is neglected but bottom friction is included. Although our model is simplified, the movements within the eddy are not constrained to be quasi-geostrophic, in the sense that the Rossby number can be relatively large and the interface surfaces at a finite distance from the center. The desired solutions are constructed analytically.

It is found that a thin lenslike eddy adjacent to a western boundary can remain in a fixed position if the current in which it is embedded is *flowing from low to high latitudes* at a ("critical") speed which depends on β, the inclination of the coastline, the frictional coefficient along the bottom of the ocean and the eddy's size, intensity and volume. Presumably, a northward flowing current whose speed is less than "critical" will allow the eddy to drift *upstream* (southward), whereas a current whose speed is stronger than the *critical* will sweep the current *downstream* (northward).

In contrast to western boundaries, thin eddies embedded in eastern longshore flows can never be stationary regardless of the current's characteristics. This difference between western and eastern boundaries exists because as the current flows, it exerts two forces on the eddy. One is parallel to the coastline (and can compensate for the eddy's β-induced force) and the other is perpendicular to the wall. In the western boundary case, the cross-stream force pushes the eddy toward the boundary causing it to lean against the wall. In the eastern boundary case, on the other hand, the force pushes the eddy away from the wall causing it to accelerate toward the open ocean.

1. Introduction

Encounters between light anticyclonic eddies and continental boundaries take place in many parts of the oceans. Examples are the Gulf Stream rings and the Loop Current eddies in the Gulf of Mexico. These encounters are inevitable because of the eddy's westward (β-induced) movement in the open ocean (e.g., Warren, 1967; Flierl, 1977; Lai and Richardson, 1977; the Ring Group, 1981; Nof, 1981b) which forces the eddies to reach the western boundaries. The question of the resulting drifts and the direction at which the eddies are migrating is of particular importance due to its relevance to the distribution of energy and properties within the ocean. In view of this, it is of interest to examine the mechanisms which might be active when an eddy drifts into the vicinity of a continent.

To illustrate some of the processes which might be active when an anticyclonic lenslike eddy comes in contact with a western wall in a resting ocean, it is recalled that the westward (β-induced) drift in the open ocean (Fig. 1) results from a balance between the southward β force and the northward Coriolis force associated with the drift (e.g., Nof, 1981b, 1983b). As the eddy encounters the wall, westward motion is, of course, no longer possible so that the northward Coriolis force, which is associated with the drift, diminishes. Consequently, the southward β force must be balanced by a new force and a new type of drift will evolve. It is expected that the eddy will start accelerating southward along the wall because the β-induced force is pointing to the south. This type of drift is quite complicated and some simplifications are, obviously, necessary in order to gain some insight into the processes in question. In view of this, we shall make two major simplifications.

First, instead of asking how an eddy adjacent to a boundary is drifting in a resting ocean, we shall focus on the conditions under which a long-shore current can balance the β-induced force and maintain the eddy in a fixed position. This eliminates the time dependency and enables one to treat a steady state problem. The above situation is probably not very common in the actual ocean because it requires a very special balance of forces. However, knowing the current which is necessary in order to keep the eddy stationary will give

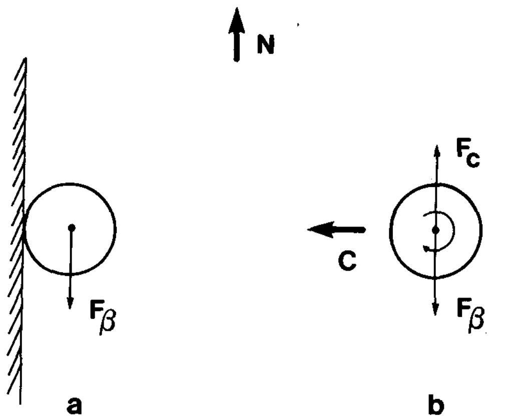

FIG. 1. Schematic diagram of the integrated forces acting on a lenslike eddy as it approaches the coast in a resting ocean. In the open ocean (b) the southward β-induced force (F_β) is balanced by the Coriolis force (F_c) which corresponds to the westward drift (see e.g., Nof, 1981b). As the eddy is approaching the coast (a) the westward drift diminishes and, consequently, the Coriolis force also diminishes. As a result, the β-induced force which is, of course, still active, is not balanced and will accelerate the eddy toward the south.

us ideas as to the direction in which the eddy will move in the presence of other currents. Second, we shall focus our attention on rather shallow eddies so that the "lift" and form drag exerted on the eddy by the fluid below is small and can be neglected. It will become clear later that this simplification essentially implies that our model can be applied to very shallow eddies such as Amazonian eddies. It cannot, however, be applied to Gulf Stream rings because their depth is of the same order as the lower layer so that their form drag cannot be neglected.

With these considerations in mind, we adopt the following situation as an idealized formulation of the problem. An isolated lenslike eddy is situated near a vertical boundary whose inclination is α (see Fig. 2). A frictional boundary current for which the details are unknown flows underneath the eddy (along the wall) and maintains the eddy in a fixed position by exerting a force that compensates for the eddy's β-induced force. We wish to determine the characteristics of this current so that we may gain insight into the mechanisms which involve the balance. As we shall see, anticyclonic eddies adjacent to a western boundary require a frictional flow from low to high latitude in order to be stationary. This suggests that anticyclonic eddies adjacent to western boundaries will have a tendency to move from high to low latitude (southward in Northern Hemisphere) in still water and that a relatively fast current is required in order to advect the eddies toward high latitudes (northward).

For simplicity it will be assumed that all the motions are hydrostatic and that the diffusion can be neglected. The upper layer contains the eddy itself which has a finite volume; the lower layer represents the boundary current and extends to infinity in both the cross-stream and longstream directions. Friction in the upper layer is neglected but the lower layer, which extends to the ocean floor, is subject to bottom stress. We shall see that it is this bottom stress which provides the balancing force that maintains the eddy in a fixed position. The coupling between the eddy and the current in which it is embedded is weak. While the eddy is influenced by the boundary current through the pressure which is directly transmitted from one region to another, the current is not affected by the presence of the eddy. This results from the fact that the eddy is rather shallow so that the perturbations introduced to the lower fluid as it flows under the eddy are negligible.

The approach which will be used in this paper is similar to that described in Nof (1981b, 1982, 1983a,b) which deals with the behavior of eddies in the open ocean. The main difference between these previous investigations and the present study is that there are now two additional forces acting on the eddy. The first results from the presence of the wall and the second from the longshore current in which the eddy is embedded. As in Nof (1981b, 1982, 1983a,b), the equations of motion are first integrated over the whole volume of the eddy so that the balances of integrated forces are obtained. When they are combined with the lower layer dynamics and a simple perturbation scheme, they provide a relationship for the speed of the boundary current and its dependency on the circulation within the eddy. In addition, the integrated relationships enable one to examine the cross-stream force exerted on the eddy by the boundary current. It turns out that, for western boundary currents, this force pushes the eddy toward the boundary causing it to lean against the wall. However, for eastern boundary currents the situation is quite different; in this case, the cross-stream force pushes the eddy away from the wall causing it to accelerate toward the open ocean. We shall see that, consequently, no eddies can be maintained in the vicinity of an eastern boundary. After presenting these general results, the model is applied to the low-salinity Amazonian eddies observed at low latitudes. Much of the discussion is devoted to a detailed examination of our assumptions and their implications.

This paper is organized as follows: the formulation of the problem is presented in Section 2 and the integrated equations in Section 3; The solution is derived in Section 4 and its analysis is presented in Section 5; Section 6 contains the applicability of our results to Amazonian eddies and Section 7 contains the analysis of our assumptions; Section 8 summarizes this work.

2. Formulation

As an idealized formulation of the problem, consider the two-layer structure shown in Fig. 2. The lenslike eddy is situated near a vertical boundary whose inclination is α. It is embedded in a boundary current

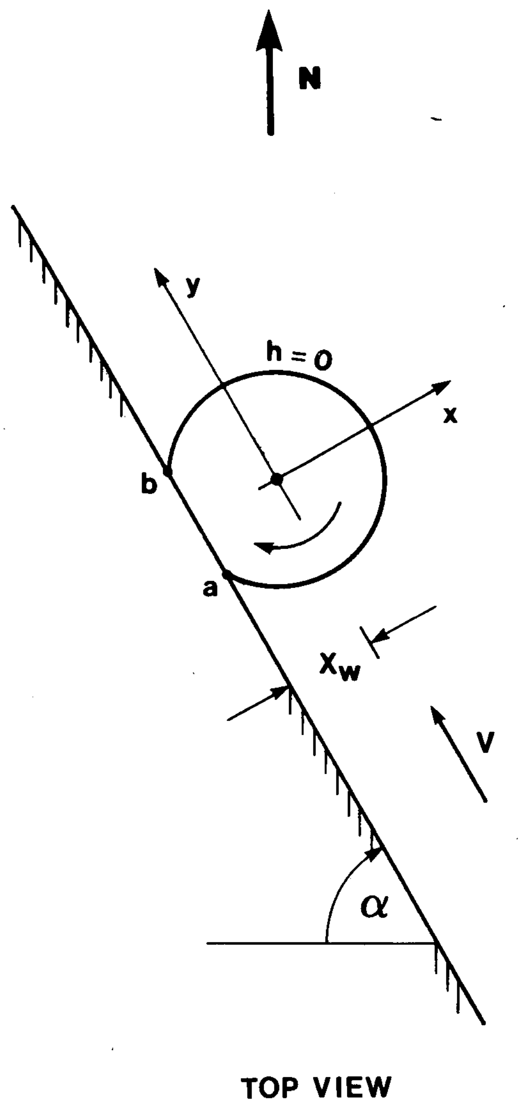

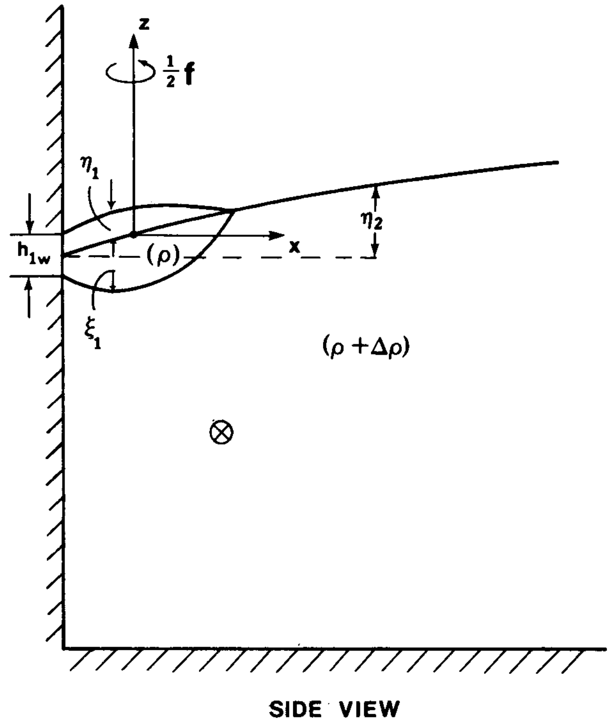

FIG. 2. Schematic diagram of the model under study. The anticyclonic eddy is situated near a vertical wall and is embedded in a longshore flow. We wish to determine the characteristics of a longshore flow that will maintain the eddy stationary. Namely, we seek a boundary current that will prevent a given eddy from drifting due to β. Here, X_w denotes the distance between the center of the eddy (i.e., where the pressure gradients and velocity vanish) and the wall. The depth of the eddy's edge is zero off the wall but finite along the wall. The free surface vertical displacements $\eta_1(x, y)$ and $\eta_2(x, y)$ are measured upward and the interface displacement $\xi_1(x, y)$ is measured downward. The density difference between the two layers is $\Delta\rho$ ($\ll\rho$) and the system rotates with an angular speed $f/2$ about the vertical axis (z). Note that the slope of the outermost streamline (i.e., the edge) is continuous in points a and b so that the speed there is not zero.

for which the undisturbed uniform depth (H) is very large compared to the eddy depth. The speed of the boundary current is to be determined; we wish to find the speed that will maintain the eddy stationary, namely—prevent it from drifting due to β. Hereafter, we shall refer to this specific speed as being the "critical" speed because it separates two different regimes. A higher speed will advect the eddy downstream whereas a lower speed will allow the eddy to drift upstream. The x-axis is chosen such that it is pointing away from the coast, and the y-axis is directed toward $270° + \alpha$ (as shown in Fig. 2) so that it is not pointing northward. This choice of coordinate system slightly complicates the representation of the Coriolis parameter but, because of the geometry, it simplifies considerably the mathematical analysis and is the most convenient system for the problem.

The flow in both layers is taken to be steady, and the pressure is assumed to be hydrostatic. Diffusion is assumed to be entirely negligible, and friction is neglected in the upper layer. The lower layer, however, is subject to bottom friction so that the boundary current loses energy as it flows from one region to another and there is a pressure drop in the downstream direction.

For hydrostatic motions, the horizontal pressure gradients depend on x and y but are independent of z; since the upper layer is inviscid, the horizontal velocity components are independent of z as well. The deviation of the hydrostatic pressure from the pressure associated with a state of rest is $\rho g(\eta_1 + \eta_2)$, and the flow within the eddy is governed by

$$u_1 \frac{\partial u_1}{\partial x} + v_1 \frac{\partial u_1}{\partial y} - [f_0 + \beta(y \sin\alpha + x \cos\alpha)]v_1 = -g\left(\frac{\partial \eta_1}{\partial x} + \frac{\partial \eta_2}{\partial x}\right), \quad (2.1)$$

$$u_1 \frac{\partial v_1}{\partial x} + v_1 \frac{\partial v_1}{\partial y} + [f_0 + \beta(y \sin\alpha + x \cos\alpha)]u_1 = -g\left(\frac{\partial \eta_1}{\partial y} + \frac{\partial \eta_2}{\partial y}\right), \quad (2.2)$$

$$\frac{\partial}{\partial x}(h_1 u_1) + \frac{\partial}{\partial y}(h_1 v_1) = 0, \quad (2.3)$$

where the subscripts 1 and 2 indicate that the variable in question is associated with the upper and lower layers respectively. Here, u_1 and v_1 are the horizontal velocity components [$u_1 = u_1(x, y)$, $v_1 = v_1(x, y)$], f_0 is the Coriolis parameter at the center of the eddy [i.e., where the pressure gradients vanish ($x = y = 0$)], $\eta_1(x, y)$ and $\eta_2(x, y)$ are the free surface vertical displacements corresponding to the upper and the lower layer movements (so that the total vertical displacement η is given by $\eta_1 + \eta_2$), g is the gravitational acceleration and h_1 the eddy depth ($\eta_1 + \xi_1$).

The density difference between the upper (ρ) and the lower layer ($\rho + \Delta\rho$) is taken to be small ($\Delta\rho \ll \rho$) and, as already mentioned, the depth of the lower layer H is assumed to be much larger than h_1. Specifically, it is assumed that the eddy is so thin (compared to the lower layer) that the flow in the lower layer remains almost unaltered as it flows beneath it. That is, there is a weak coupling between the eddy and the environmental fluid. Although the eddy is influenced by the mean flow, there is no influence of the eddy on the surrounding fluid. The validity of this assumption will be examined in detail in Section 7. It will then become clear that the conditions necessary for this assumption to be valid are satisfied by some, but not all, eddies of practical interest. For instance, we shall see that the assumption is valid for Amazonian eddies which (due to their proximity to the equator) are very shallow (~10 m) but is not valid for Gulf Stream rings which are relatively deep (~600 m).

Under the conditions mentioned above, the eddy introduces negligible pressure gradients in the fluid below so that the interface displacement $\xi_1(x, y)$ (measured downward from the free surface) is given by

$$\xi_1 = \frac{\rho}{\Delta\rho}\eta_1, \quad (2.4)$$

and h_1, the total eddy's depth, can be approximated by ξ_1 without introducing errors larger than $O(\Delta\rho/\rho)$.

Equations (2.1)–(2.3) are subject to the boundary conditions

$$h_1 = 0; \quad \phi(x, y) = 0; \quad x > -x_w, \quad (2.5a)$$

$$h_1 = h_{1w}; \quad y_{wa} \leqslant y \leqslant y_{wb}; \quad x = -x_w, \quad (2.5b)$$

$$(u_1\mathbf{i} + v_1\mathbf{j}) \cdot \nabla\phi = 0; \quad \phi(x, y) = 0; \quad x > -x_w, \quad (2.5c)$$

$$u_1 = 0; \quad y_{wa} \leqslant y \leqslant y_{wb}; \quad x = -x_w, \quad (2.5d)$$

where ∇ is the horizontal del operator and the subscript w denotes that the variable in question is associated with the wall. The first condition (2.5a) states that off the wall, $h_1 = 0$ along a curve which is not known in advance (ϕ) and the second condition (2.5b) reflects the fact that along the wall [i.e., between points (a) and (b) shown in Fig. 2], the depth h_{1w} is not necessarily zero. It will be seen shortly that the latter condition results from the fact that the eddy is pressed against the wall. Conditions (2.5c) and (2.5d) imply that the eddy's edge is a streamline both off and along the wall. These conditions correspond to the fact that the location and shape of the eddy's edge are not known in advance but rather must be determined as part of the problem. Note that $\partial p/\partial x$ and $\partial p/\partial y$ are continuous at points a and b (Fig. 2) so that the velocity does not vanish there.

Since the lower layer is flowing along the coast, it is assumed that its streamline's radius of curvature is very large so that the nonlinear terms can be neglected. We shall see later that, for our lower layer, the nonlinear terms are identically zero so that the assumption is certainly adequate. In a similar fashion to Stommel's frictional model (Stommel, 1948; Veronis, 1966, 1981), the (flat) bottom stress is taken to be linearly proportional to the speed so that the vertically integrated governing equations are

$$[f_0 + \beta(y \sin\alpha + x \cos\alpha)]V = g\frac{\partial \eta_2}{\partial x} + KU, \quad (2.6)$$

$$[f_0 + \beta(y \sin\alpha + x \cos\alpha)]U = -g\frac{\partial \eta_2}{\partial y} - KV, \quad (2.7)$$

$$U_x + V_y = 0. \quad (2.8)$$

Here,

$$V = \frac{1}{H}\int_{-H}^{0} v_2 dz, \quad U = \frac{1}{H}\int_{-H}^{0} u_2 dz,$$

and the frictional coefficient K is typically 2×10^{-6} s^{-1} (see e.g., Veronis, 1981).

The system (2.6)–(2.8) is subject to the boundary conditions

$$U = 0; \quad x = -x_w; \quad -\infty < y < \infty, \quad (2.9)$$

$$U, V < M; \quad x \rightarrow \infty; \quad -\infty < y < \infty, \quad (2.10)$$

where M is an arbitrary constant. Condition (2.9) states that the wall is a streamline and (2.10) reflects the fact that the velocities must be bounded at infinity.

In order to bring out some of the properties which will be useful for an understanding of the complete problem, we shall now examine the structure that the eddy would have on an f-plane. This f-plane state will later be used as a basic state for our perturbation scheme; namely, it will be taken to be the zeroth-order solution. When $\beta \rightarrow 0$, the governing equations for the upper and lower layers reduce to

$$\bar{u}_1 \frac{\partial \bar{u}_1}{\partial x} + v_1 \frac{\partial \bar{u}_1}{\partial y} - f_0\bar{v}_1 = -g'\frac{\partial \bar{h}_1}{\partial x} - g\frac{\partial \bar{\eta}_2}{\partial x}, \quad (2.11)$$

$$\bar{u}_1 \frac{\partial \bar{v}_1}{\partial x} + \bar{v}_1 \frac{\partial \bar{v}_1}{\partial y} + f_0 \bar{u}_1 = -g' \frac{\partial \bar{h}_1}{\partial y} - g \frac{\partial \bar{\eta}_2}{\partial y}, \quad (2.12)$$

$$\frac{\partial}{\partial x}(\bar{h}_1 \bar{u}_1) + \frac{\partial}{\partial y}(\bar{h}_1 \bar{v}_1) = 0, \quad (2.13)$$

$$f_0 \bar{V} = g \frac{\partial \bar{\eta}_2}{\partial x} + K\bar{U}, \quad (2.14)$$

$$f_0 \bar{U} = -g \frac{\partial \bar{\eta}_2}{\partial y} - K\bar{V}, \quad (2.15)$$

$$\bar{U}_x + \bar{V}_y = 0, \quad (2.16)$$

where condition (2.4) has been used to express the pressure gradient term in the upper layer and the overbar is used to indicate that the variable in question is associated with the f-plane state. In Section 4, the overbar will be replaced by (0) to indicate its association with the zeroth-order state. The boundary conditions remain the same [(2.5a)–(2.5d), (2.9), (2.10)] so that even on an f-plane the eddy's shape is unknown and should be determined as part of the problem.

The solution for the lower layer is

$$\bar{V} = \bar{U} = \bar{\eta}_2 = 0, \quad (2.17)$$

and for the upper layer, one finds that any radially symmetric swirl speed [i.e., $\bar{v}_\theta = \bar{v}_\theta(r)$, $\bar{h}_1 = \bar{h}_1(r)$, $\partial/\partial\theta = 0$, $\bar{v}_r = 0$] satisfies the equations and boundary conditions when $\bar{x}_w = -r_0$; $\bar{h}_{1w} = 0$; $\bar{y}_{wa} = \bar{y}_{wb} = 0$. This can be easily demonstrated by substituting (2.17) into (2.11)–(2.13) and writing the resulting equations in polar coordinates which, with $\partial/\partial\theta = 0$ and $\bar{v}_r = 0$, reduce to the single equation

$$\frac{\bar{v}_\theta^2}{r} + f_0 \bar{v}_\theta = g' \frac{\partial \bar{h}_1}{\partial r}. \quad (2.18)$$

For any $\bar{v}_\theta(r)$, one can find the solution for $\bar{h}_1(r)$ so that any radially symmetric structure for $\bar{v}_\theta$ satisfies (2.11)–(2.13) as stated above.

In view of these, the properties of the solution on an f-plane (Fig. 3) can be summarized as follows:

1) The eddy is stationary with a resting lower layer ($\bar{V} = \bar{U} = 0$); in other words, the critical speed is zero.
2) The eddy has a circular structure and the shape of its edge corresponds to an exact circle.
3) The eddy touches the boundary at a point.

The internal eddy's structure and the dependence of the swirl velocity on r can be determined by various methods such as specifying the velocity or potential vorticity and finding the remaining variables. This point will be further discussed in Sections 5 and 6.

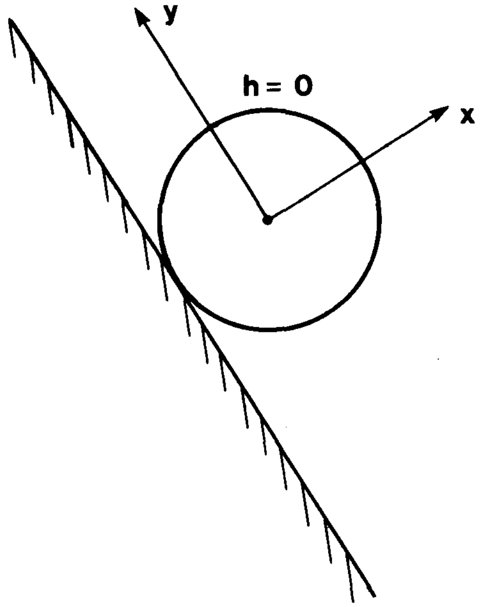

FIG. 3. Schematic diagram of an eddy on an f-plane situated near a vertical boundary. The eddy is circular and its outer edge touches the boundary at a point. Obviously, no boundary current is required in order to maintain the eddy in a fixed position (i.e., $V = 0$).

3. General balance of forces

To obtain the general solution to the problem (i.e., the behavior of the eddy on a β-plane) (2.2) is integrated over the whole volume of the eddy:

$$\iiint \left(u_1 \frac{\partial v_1}{\partial x} + v_1 \frac{\partial v_1}{\partial y}\right) dxdydz + \iiint [f_0 + \beta(y \sin\alpha + x \cos\alpha)] u_1 dxdydz = -\iiint \left(g' \frac{\partial h_1}{\partial y} + g \frac{\partial \eta_2}{\partial y}\right) dxdydz, \quad (3.1)$$

where, as before, condition (2.4) has been used to express the pressure gradient term. Since u_1 and v_1 are independent of z, (3.1) reduces to

$$\iint_S \left(h_1 u_1 \frac{\partial v_1}{\partial x} + h_1 v_1 \frac{\partial v_1}{\partial y}\right) dxdy + \iint_S [f_0 + \beta(y \sin\alpha + x \cos\alpha)] u_1 h_1 dxdy = -\iint_S \left(\frac{g'}{2} \frac{\partial (h_1^2)}{\partial y} + g h_1 \frac{\partial \eta_2}{\partial y}\right) dxdy, \quad (3.2)$$

where S is the projection of the eddy's outer surface on the x,y-plane. Using (2.3) and Stokes' theorem, one can express (3.2) as

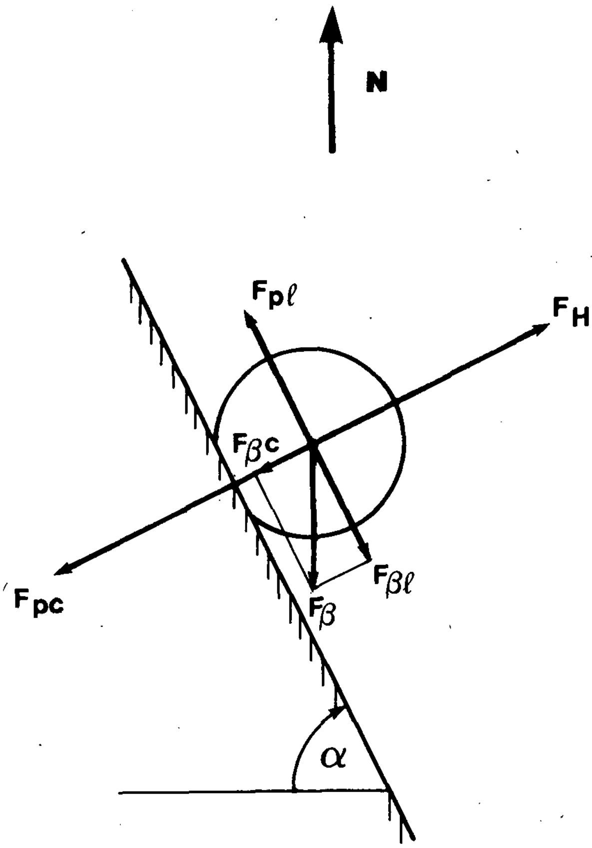

FIG. 4. A schematic diagram of the balance of forces associated with a stationary lenslike eddy near a western wall. The southward β-induced force (F_β) has two components, a long-stream component ($F_{\beta\ell}$) and a cross-stream component ($F_{\beta c}$). The long-stream component ($F_{\beta\ell}$) is balanced by the downstream pressure gradient imposed on the eddy by the lower layer ($F_{p\ell}$). Note that the latter results from bottom friction which forces a long-stream pressure drop. In the cross-stream direction, the β-force component ($F_{\beta c}$) and the pressure force exerted by the lower layer (F_{pc}) are balanced by a hydrostatic force (F_H) which results from the direct contact between the eddy and the wall.

$$-\int_{\tilde\phi} h_1 v_1^2 dx + \int_{\tilde\phi} h_1 u_1 v_1 dy + \iint_S [f_0 + \beta(y \sin\alpha + x \cos\alpha)] u_1 h_1 dxdy = \frac{g'}{2}\int_{\tilde\phi} h_1^2 dx - g \iint_S h_1 \frac{\partial \eta_2}{\partial y} dxdy, \quad (3.3)$$

where $\tilde\phi$ denotes the eddy's outer boundary which includes both the section along the wall and the section off the wall (where $h_1 = 0$). Since $\tilde\phi$ is a streamline (i.e., $u_1 dy = v_1 dx$ along $\tilde\phi$), the integrals of the nonlinear terms vanish identically. With the aid of the transport function

$$\frac{\partial \psi_1}{\partial y} = -u_1 h_1; \quad \frac{\partial \psi_1}{\partial x} = v_1 h_1, \quad (3.4)$$

the resulting equation can be written in the form

$$-f_0 \iint_S \frac{\partial \psi_1}{\partial y} dxdy - \beta \sin\alpha \iint_S \frac{\partial}{\partial y}(y\psi_1) dxdy - \beta \cos\alpha \iint_S \frac{\partial}{\partial y}(x\psi_1) dxdy + \beta \sin\alpha \iint_S \psi_1 dxdy = \frac{g'}{2}\int_b^a h_{1w}^2 dx - g \iint_S h_1 \frac{\partial \eta_2}{\partial y} dxdy, \quad (3.5)$$

where h_{1w} is the depth along the wall and we have taken into account that, off the wall, $h_1 = 0$ along the edge ($\tilde\phi$). By choosing ψ_1 to be zero along $\tilde\phi$, noting that $dx = 0$ along the wall and using Stokes' theorem again, (3.5) can be further reduced to

$$g \iint_S h_1 \frac{\partial \eta_2}{\partial y} dxdy = -\beta \sin\alpha \iint_S \psi_1 dxdy. \quad (3.6)$$

This equation represents the balance of forces parallel to the wall [i.e., in the y-direction (see Figs. 4 and 5)]. It states that the y-component of the β-induced force is balanced by the downstream pressure gradient of the lower layer which is directly transmitted to the eddy.

By repeating the procedure outlined above and applying the same techniques to (2.1), one finds the balance of integrated forces perpendicular to the wall such that

$$F = \underbrace{\beta \cos\alpha \iint_S \psi_1 dxdy}_{\text{I}} + \underbrace{g \iint_S h_1 \frac{\partial \eta_2}{\partial x} dxdy}_{\text{II}}, \quad (3.7)$$

where

$$F = \frac{g'}{2}\int_a^b h_{1w}^2 dy$$

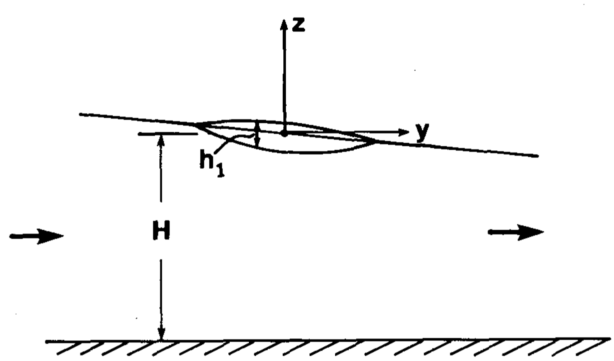

FIG. 5. Schematic diagram of the sea level along the current and the eddy. As a result of bottom friction, the longshore current loses energy and its sea level drops as it flows from low to high latitudes. This drop in sea level is directly transmitted to the eddy and compensates for the southward β-induced force (see text).

represents the hydrostatic force exerted on the eddy by the wall. This force balances the component of the β-force (see Fig. 4) which presses the eddy toward the wall (I) and the cross-stream pressure force exerted by the lower layer on the eddy (II). It must be larger than zero because otherwise, there would not be any direct contact between the eddy and the boundary. That is to say, if the right-hand side of (3.7) is negative [(I + II) < 0], then the eddy would be accelerating away from the wall because there is no steady force which can balance it. We shall see later that for western boundaries, $F > 0$ (as required) but for eastern boundaries, $F < 0$ indicating that thin isolated eddies cannot persist near an eastern wall. Before continuing, it is worth mentioning that the detailed numerical value of F (save for its sign) is of no importance to our analysis because all the desired information can be obtained from (3.6).

4. Solution

a. Scaling

In the subsequent analysis the following upper layer nondimensional variables will be used:

$$x^* = 2x/\ell_1; \quad y^* = 2y/\ell_1; \quad u_1^* = 2u_1/\mathrm{Ro}f_0\ell_1$$
$$v_1^* = 2v_1/\mathrm{Ro}f_0\ell_1; \quad \psi_1^* = 6\psi_1/\mathrm{Ro}f_0\ell_1^2\hat{h}_1;$$
$$R_d = (g'\hat{h}_1)^{1/2}/f_0$$
$$h_1^* = h_1/\hat{h}; \quad \eta_1^* = 2\eta_1/(\mathrm{Ro}f_0^2\ell_1^2g^{-1}). \tag{4.1}$$

Here, ℓ_1 is the eddy size (defined as half the distance between the northernmost and southernmost edges), R_d the internal deformation radius, Ro the Rossby number, and $\hat{h}_1 = h_1(0, 0)$. The numerical coefficients in (4.1) have been introduced for convenience; by defining the nondimensional variables in this particular way, the subsequent expansion will correspond to the actual ratio between the perturbations and the basic state.

For the lower layer the nondimensional variables should be defined in a somewhat different way because the length scale in the y-direction is not identical to the eddy size (ℓ_1) due to the presence of bottom stress and the weak coupling between the two layers. The lower layer scale in the x-direction can be taken, for convenience, to be identical to the eddy's size (ℓ_1). However, since the lower layer is not affected by the eddy's depth there are two choices for the length scale in the y-direction.

The first is the radius of the earth which corresponds to the scale measuring the change in the boundary current due to β. The second, which as we shall see shortly is more appropriate for our problem, is the scale which corresponds to a pressure drop similar to that which would occur over a distance ℓ_1 in the x-direction. The latter is given by $\ell_1 f_0/K$ because the sea level change across the eddy in the x-direction is $\sim O(fV\ell_1/g)$ and the balance in the y-direction is expected to be between the frictional terms and the pressure term. That is, $\ell_1 f_0/K$ is the y-scale along which there will be a sea level drop similar to that occurring across the eddy. Since K is usually at least an order of magnitude smaller than f_0, the frictional scale in the y-direction is an order of magnitude larger than the scale in the x-direction. This is in agreement with our general assumption regarding the structure of the lower layer because it corresponds to the characteristics of a boundary current. It is easy to choose between the two length scales in the y-direction because the radius of the earth is $\sim$6000 km, whereas the frictional length scale is considerably smaller—usually $\sim$1000 km (for $\ell_1 \sim 100$ km). Hence, the frictional length scale is the more appropriate choice for our problem.

In view of these considerations, we define the following nondimensional variables for the lower layer,

$$x^* = 2x/\ell_1; \quad y^* = 2yK/\ell_1 f_0; \quad V^* = 2V/\mathrm{Ro}f_0\ell_1$$
$$U^* = 2U/\mathrm{Ro}\ell_1 K; \quad \eta_2^* = 2\eta_2/(\mathrm{Ro}f_0^2\ell_1^2g^{-1}). \tag{4.2}$$

We also introduce a "frictional beta number" which involves parameters of both layers and is defined as

$$\epsilon = \left(\frac{\beta\ell_1}{6K}\right) \ll 1. \tag{4.3}$$

It will become clear later that all the nondimensional numbers and their associated numerical coefficients have been defined in such a way that ϵ represents the actual ratio between the critical longshore current speed and the eddy's orbital velocity.

We shall focus our attention on eddies for which the parameters satisfy

$$(x^*, y^*) \sim O(1); \quad (u_1, v_1) \sim O(1); \quad \psi_1^* \sim O(1)$$
$$\epsilon \sim O\left(\frac{K}{f_0}\right) \sim O(10^{-1}); \quad h_1^* \sim O(1);$$
$$\eta_2^* \sim O(\epsilon), (U^*, V^*) \sim O(\epsilon). \tag{4.4}$$

We shall see in Sections 6 and 7 that these scales are appropriate for Amazonian eddies.

In terms of the nondimensional variables defined by (4.1)–(4.3), the integrated equations for the upper layer (3.6)–(3.7) are

$$\epsilon \sin\alpha \iint_{S^*} \psi_1^* dx^* dy^* = -\iint_{S^*} h_1^* \frac{\partial \eta_2^*}{\partial y^*} dx^* dy^*, \tag{4.5}$$

$$F^* = \iint_{S^*} h_1^* \frac{\partial \eta_2^*}{\partial x^*} dx^* dy^* + \epsilon\left(\frac{K}{f_0}\right) \cos\alpha \iint_{S^*} \psi_1^* dx^* dy^*, \tag{4.6}$$

where F^*, the force exerted on the eddy in the direction perpendicular to the wall, has been nondimensionalized by $(\hat{h}\,\mathrm{Ro} f_0 \ell_1{}^3/4)$ and $\partial\eta_2/\partial y$; $\partial\eta_2/\partial x$ have been nondimensionalized taking into account that they are associated with the lower layer.

By substituting (4.2)–(4.3) into (2.6)–(2.8), one finds that the nondimensional equations governing the lower layer are

$$\left\{1 + 3\epsilon\left[y^* \sin\alpha + \left(\frac{K}{f_0}\right)x^* \cos\alpha\right]\right\}V^* = 2\frac{\partial\eta_2^*}{\partial x^*} + \left(\frac{K}{f_0}\right)^2 U^*, \quad (4.7)$$

$$\left\{1 + 3\epsilon\left[y^* \sin\alpha + \left(\frac{K}{f_0}\right)x^* \cos\alpha\right]\right\}U^* = -2\frac{\partial\eta_2^*}{\partial y^*} - V^*, \quad (4.8)$$

$$\frac{\partial U^*}{\partial x^*} + \frac{\partial V^*}{\partial y^*} = 0. \quad (4.9)$$

b. Perturbation analysis

It is further assumed that all the dependent variables possess power series expansions in ϵ, e.g.,

$$\begin{aligned} v_1^* &= v_1^{(0)} + \epsilon v_1^{(1)} + \cdots, \\ \eta_2^* &= \epsilon\eta_2^{(1)} + \epsilon^2\eta_2^{(2)} + \cdots \\ V^* &= \epsilon V^{(1)} + \epsilon^2 V^{(2)} + \cdots, \\ F^* &= \epsilon F^{(1)} + \epsilon^2 F^{(2)} + \cdots, \end{aligned} \quad (4.10)$$

where the zeroth-order state corresponds to the solution on an f-plane ($\beta \to 0$, $\epsilon \to 0$) discussed earlier in Section 2. That is, it is assumed that since the parameter which involves β is small, the perturbations induced by the presence of β are also small so that the structure of the eddy will only slightly deviate from the f-plane structure. We shall see later that the first-order longshore flow $V^{(1)}$, $U^{(1)}$ can be found without finding the complete detailed solution for the flow within the eddy. The detailed solution for the flow within the eddy will be left as a subject for future investigation.

By substituting (4.10) into (4.5)–(4.9), one finds the following equations for the first-order variables,

$$\sin\alpha \iint_{S^{(0)}} \psi_1^{(0)} dx^* dy^* = -\iint_{S^{(0)}} h_1^{(0)} \frac{\partial\eta_2^{(1)}}{\partial y^*} dx^* dy^*, \quad (4.11)$$

$$F^{(1)} = \iint_{S^{(0)}} h_1^{(0)} \frac{\partial\eta_2^{(1)}}{\partial x^*} dx^* dy^*, \quad (4.12)$$

$$V^{(1)} = \frac{2\partial\eta_2^{(1)}}{\partial x^*}, \quad (4.13)$$

$$U^{(1)} = \frac{2\partial\eta_2^{(1)}}{\partial y^*} - V^{(1)}, \quad (4.14)$$

$$\frac{\partial U^{(1)}}{\partial x^*} + \frac{\partial V^{(1)}}{\partial y^*} = 0, \quad (4.15)$$

where $S^{(0)}$ is the surface area that the eddy would have on an f-plane. The solution of (4.13)–(4.15) which satisfies the boundary conditions (2.9)–(2.10) is simply

$$U^{(1)} = 0;$$

$$V^{(1)} = 2\frac{\partial\eta_2^{(1)}}{\partial x^*} = -2\frac{\partial\eta_2^{(1)}}{\partial y^*} = \text{constant}. \quad (4.16)$$

Namely, the flow in the lower layer is uniform and geostrophic in the cross-stream direction. It is directed down the pressure gradient up to high latitude because along the stream the balance is between frictional and pressure forces.

Equation (4.16) can be directly substituted into (4.11)–(4.12) to give

$$V^* = 2\epsilon \sin\alpha \iint_{S^{(0)}} \psi_1^{(0)} dx^* dy^* \Big/ \iint_{S^{(0)}} h_1^{(0)} dx^* dy^* + O(\epsilon^2) + \cdots, \quad (4.17)$$

$$F^* = 2\epsilon \sin\alpha \iint_{S^{(0)}} \psi_1^{(0)} dx^* dy^* + O(\epsilon^2) + \cdots. \quad (4.18)$$

Because the zeroth-order state is always radially symmetric, it is convenient to express (4.17)–(4.18) in polar coordinates; for clarity we shall subsequently use the polar variables in dimensional form. In these variables, (4.17)–(4.18) are

$$V = \frac{\beta f_0 \sin\alpha}{K} \int_0^{r_0} \int_{r_0}^{r} \bar{v}_\theta(\tilde{r})\bar{h}_1(\tilde{r}) d\tilde{r} r dr \Big/ \int_0^{r_0} \bar{h}_1(r) r dr + O\left[\left(\frac{\beta r_0}{6K}\right)^2 \bar{v}_\theta\right], \quad (4.19)$$

$$F = \frac{\beta f_0 \sin\alpha}{K} \int_0^{r_0} \int_{r_0}^{r} \bar{v}_\theta(\tilde{r})\bar{h}_1(\tilde{r}) d\tilde{r} r dr + O\left[\left(\frac{\beta r_0}{6K}\right)^2 f_0 \bar{v}_\theta \hat{h}_1 r_0^2\right], \quad (4.20)$$

where, as before, $\bar{v}_\theta(r)$ and $\bar{h}_1(r)$ are the dimensional swirl velocity and depth corresponding to the basic state ($\beta \to 0$, $\epsilon \to 0$) and r_0 is the dimensional radius of the eddy corresponding to the same state [$\bar{h}_1(r_0) = 0$].

Before discussing the implications of our results, it should be pointed out that the existence of an equilibrium state corresponding to the balance given by

(4.19) and (4.20) also requires vanishing of the moment of momentum [see e.g., Shen (1981)]. It is easy to show that the integrated moment of momentum is satisfied to $O(\epsilon)$ as required.

5. Analysis

Relation (4.19) and (4.20) enable one to compute the critical longshore current speed provided that the swirl velocity and depth (associated with the f-plane structure) are known. For simplicity, we shall follow the analysis of Nof (1981b) and Killworth (1983) and consider eddies whose basic state corresponds to a linear velocity profile, i.e.,

$$\bar{v}_\theta = -\mathrm{Ro} f_0 r. \tag{5.1}$$

This velocity structure is not only convenient but also corresponds to the structure that Amazonian eddies are expected to have. With Ro = 1/2, (5.1) corresponds to zero potential vorticity which is the expected vorticity of Amazonian eddies since they originate from the equator where both the relative and planetary vorticity are approximately zero [see Nof (1981a), 26–27]. The depth of the eddy $[\bar{h}_1(r)]$ is found, by integrating the nonlinear momentum equation (2.18), to be

$$\bar{h}_1(r) = \hat{h}_1 + \mathrm{Ro} f_0^2 r^2(\mathrm{Ro} - 1)/2g', \tag{5.2}$$

where, as before, $\hat{h}_1$ denotes the maximum depth (at $r = 0$). Eq. (5.2) shows that the interface strikes the free surface ($\bar{h}_1 = 0$) along the circle

$$r_0 = \left[\frac{2g'\hat{h}_1}{\mathrm{Ro}(1 - \mathrm{Ro})}\right]^{1/2} f_0^{-1}. \tag{5.3}$$

Note that there is an upper bound to the degree of nonlinearity which can be associated with (5.1) because the relative vorticity

$$\frac{1}{r}\frac{r}{dr}(r\bar{v}_\theta)$$

cannot be larger than f_0. Consequently, the largest Rossby number which can be associated with (5.1)–(5.3) is 1/2.

The critical speed of the longshore current is now found, by substituting (5.1)–(5.3) into (4.19), to be:

$$V = \beta f_0 R_d^2 \sin\alpha/3(1 - \mathrm{Ro})K + O[\beta^2 r_0^2 \bar{v}_\theta/36K^2], \tag{5.4}$$

which, in view of (5.3), can also be expressed in the form

$$V = \beta f_0 \,\mathrm{Ro} r_0^2 \sin\alpha/6K + O[\beta^2 r_0^2 \bar{v}_\theta/36K^2]. \tag{5.4a}$$

Hence, the ratio between the perturbed velocity (V) and the basic state speed ($-\mathrm{Ro} f_0 r_0$) is $\beta r_0 \sin\alpha/6K$, which equals the parameter ϵ times $\sin\alpha$. This supports our definition of the nondimensional variables. Note that, for a fixed deformation radius, V increases with nonlinearity and decreases with increasing the frictional coefficient K. This results from the fact that an increased swirl speed causes an increase in the β-induced force which, in turn, requires a larger critical speed or a larger frictional coefficient.

By substituting (5.1)–(5.3) into (4.20), one finds that the cross-stream force exerted on the eddy by the longshore current is

$$F \approx \frac{\beta f_0 R_d^4 \hat{h}_1 f_0 \sin\alpha}{6K\,\mathrm{Ro}(1 - \mathrm{Ro})^2}. \tag{5.5}$$

As already mentioned, this force is acting in the direction perpendicular to the wall; to examine its role, it is recalled that α is measured clockwise from the western direction so that $\alpha < \pi$ for western boundaries and $\alpha > \pi$ for eastern boundaries. For western boundary currents ($F > 0$, see Fig. 6), the force is pushing the eddy against the wall and is, therefore, balanced by a hydrostatic pressure force

$$\left(\frac{g'}{2}\int_a^b h_{1w}^2 dy\right)$$

resulting from the direct contact between the eddy and the wall. However, when $\alpha > \pi$ (eastern boundary), this force is pointing toward the open ocean so that it cannot be balanced by a hydrostatic force and, consequently, it pushes the eddy away from the wall. We conclude, therefore, that in the vicinity of an eastern boundary, there is no longshore current which can maintain the eddy in a fixed position. When $\alpha \to 0$, π, our perturbation analysis breaks down because terms which have been ignored (by the perturbation analysis) as small [e.g., the second term on the right-hand side of (4.6)] are no longer negligible.

6. Application to Amazonian eddies

In this section we shall discuss the applicability of our model to the low salinity lenses which are found in low latitudes (Fig. 7) and originate from the Amazon river at the tropics.

Following Ryther *et al.* (1967), Gibbs (1970) and Nof (1981a), we choose the following values as being typical for the parameters associated with Amazonian eddies:

$$\ell_1 \sim 100\ \mathrm{km};\quad f_0 \sim 1.7\times10^{-5}\ \mathrm{s^{-1}};$$
$$\beta \sim 2\times10^{-11}\ \mathrm{m^{-1}\,s^{-1}};$$
$$\hat{h} \sim 8\ \mathrm{m};\quad g' \sim 0.1\ \mathrm{m\,s^{-2}};\quad \alpha \sim 45°. \tag{6.1}$$

Because of the eddies' proximity to the equator, they are extremely shallow and their density is smaller than that of most mesoscale eddies in the ocean. Their core's salinity can be as low as 24‰ [corresponding to $\Delta\rho/\rho \sim O(10^{-2})$] and most of their area is situated above deep water [$H \sim 5000$ m].

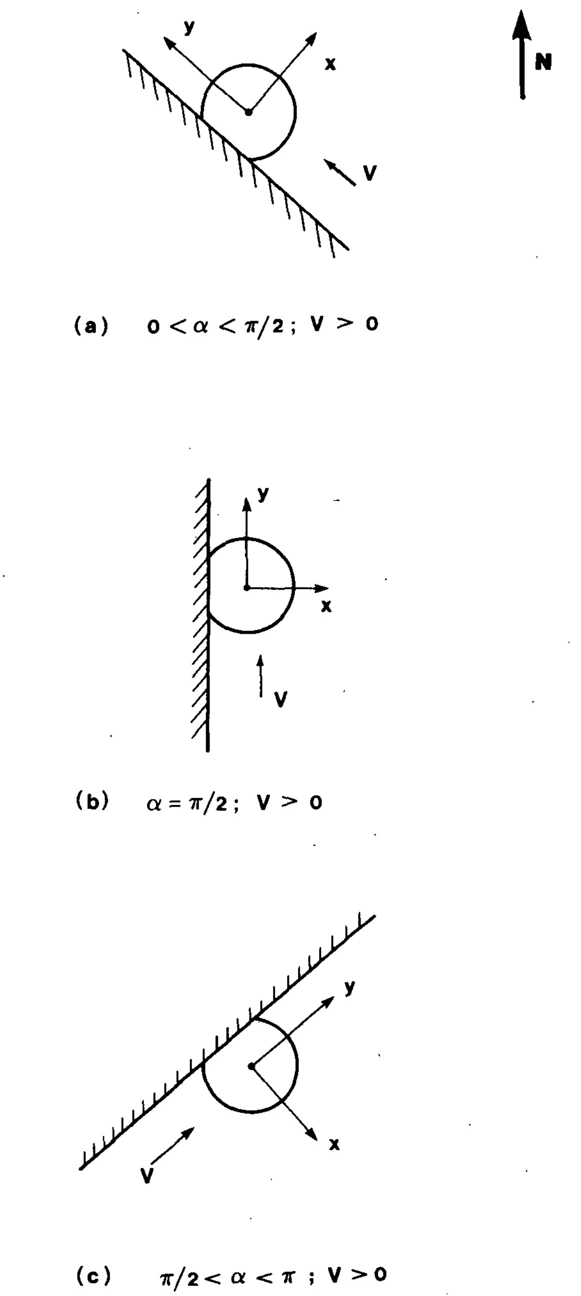

FIG. 6. A sketch of the possible situations associated with stationary anticyclonic eddies embedded in critical western boundary currents. For all angles between zero and π ($0 < \alpha < \pi$), a flow from low to high latitudes is required in order to maintain the eddy stationary.

In order to apply our model to these eddies we shall take the frictional coefficient K to be $2 \times 10^{-6}\ \mathrm{s}^{-1}$. Very similar values were used by Veronis (1981), Veronis (1966) and Stommel (1948) who examined the general circulation in the North Atlantic. As pointed out by Rooth (1972), such a numerical value for K is probably not simply related to the actual stress at the bottom but, nevertheless, it is adequate for the use in vertically integrated equations. With this frictional coefficient and the numerical values given by (6.1) the expansion parameter ϵ is O(0.1).

To obtain the critical speed for Amazonian eddies, we take Ro = 1/2 [because, as mentioned before, it corresponds to zero potential vorticity], the chosen value of K discussed earlier [$2 \times 10^{-6}\ \mathrm{s}^{-1}$] and the numerical values given by (6.1) and substitute these into (5.4) giving

$$V = \frac{2}{3}\frac{\beta f_0 R_d^2}{K}\sin\alpha \approx 0.2\ \mathrm{m\ s^{-1}}. \qquad (6.2)$$

This critical speed corresponds to an eddy with a predicted radius (r_0) of $\sim$150 km [obtained from (6.1) and (5.3) with Ro = 1/2] and a maximum swirl speed [$\frac{1}{2}f_0 r_0$] of 1.2 m s^{-1}. The predicted radius agrees with the observations (see e.g., Fig. 7) but there are no direct measurements to support (or reject) our prediction of the swirl speed. The predicted speed is, however, in agreement with the speed of other lenslike eddies in the ocean [see e.g., Csanady (1979)] so that it is probably not very far from the actual value.

Our results suggest that a northwestern current of $\sim$0.2 m s^{-1} is required in order to keep the eddy stationary near the coast. Presumably, a stronger current will sweep the eddy toward the northwest, whereas a weaker current will allow the eddy to drift toward the southeast. The Guiana current's speed is $\sim$1 m s^{-1} [see e.g., Gorshkov (1978)], much faster than the critical speed ($\sim$0.2 m s^{-1}), so that it is expected that the current will carry the eddies toward the Caribbean Sea. This suggested behavior is supported by a number of investigations which have pointed out that low salinity Amazonian eddies arrive downstream at Barbados [Borstad (1982a,b), Landis (1971)] several times during the year. This suggestion is perhaps not very surprising and could probably be expected because the Guiana current is very fast and a relatively strong force is needed in order to oppose it. Nevertheless, it illustrates that in the absence of such a current the eddies would have a tendency to drift southward so that they could never reach the eastern Caribbean. Apart from the critical speed and its consequences, our model also suggests that the eddies are pushed against the wall (Fig. 6). As a result, it is expected that the eddy's edge near the wall will have a tendency to adjust itself to the shape of the coast. This is clearly supported by the observed shape (Fig. 7) which illustrates that the eddy is indeed leaning against the coast.

So far we have focused on the details of our model and its applicability to Amazonian eddies but we have not yet examined the validity of our assumptions. This is done in the next section where it is shown that all our assumptions are consistent with the scales of Amazonian eddies.

7. Limitations and validity of assumptions

In this section we shall examine the validity of our various approximations and discuss the weaknesses of

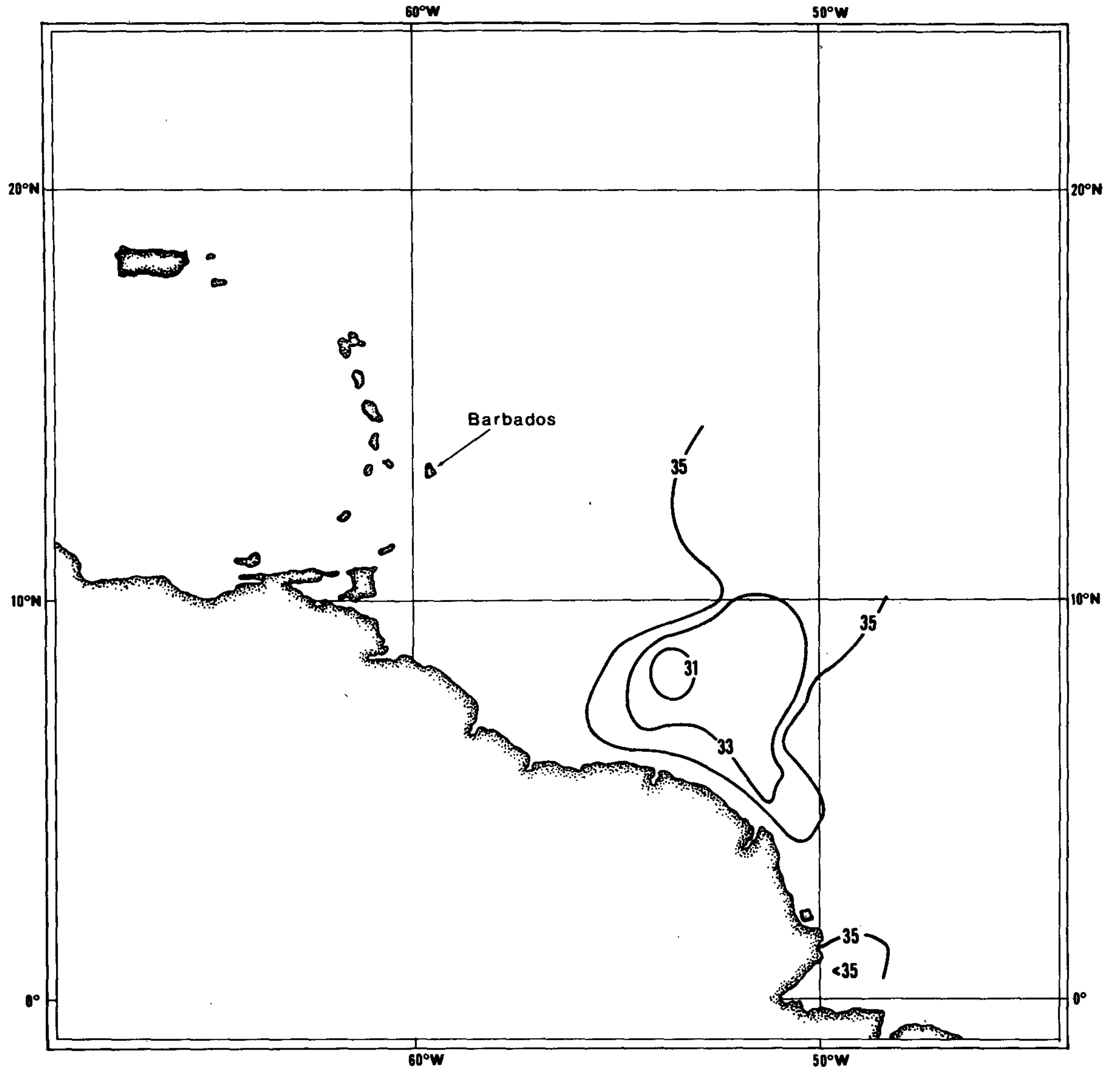

FIG. 7. Surface salinity contours for *Atlantis II* Cruise 14 (October–December 1964) [adapted from Ryther *et al.* (1967)]. Note that the eddy is situated near the boundary and appears to be pushed toward the wall in a manner similar to that suggested by our model (see Figs. 2, 4 and 6). It is suggested that this behavior and the frequent observations of Amazonian eddies near Barbados are a result of the Guiana Current which flows toward the northwest (see text) at a speed higher than that required for stationarity.

our proposed model. We shall begin by examining the assumption regarding the neglect of form drag and "lift" exerted on the eddy by the lower layer.

To do so, it is recalled that the lower layer is affected by the presence of the eddy in a similar fashion to that of a single layer flowing above an obstacle. We can, therefore, estimate the disturbances introduced to the lower layer and the resulting form drag by looking at the inviscid potential vorticity equation for the lower layer

$$\frac{D}{Dt}\left(\frac{\tilde{v}_x - \tilde{u}_y + f}{h}\right) = 0$$

(where $\tilde{u}$ and $\tilde{v}$ are the perturbations). This equation illustrates that the disturbances introduced to the lower layer by the presence of the eddy ("bump") are

$$\tilde{u}, \tilde{v} \sim O\left(f_0 \frac{\hat{h}_1}{H} \ell_1\right). \qquad (7.1)$$

In order for the form drag to be negligible, it is necessary that the left-hand side of (2.7) (as well as the nonlinear terms) be small compared to the frictional term (KV). Under such conditions, the scales that have been introduced for the lower layer (4.2) are indeed the correct ones. Since the cross-stream velocities introduced by the eddy are, at the most, of the order $f_0\ell_1\hat{h}_1/H$, we find that the neglect of form drag and lift is justified as long as

$$KV \gg f_0^2 \frac{\hat{h}_1}{H} \ell_1. \tag{7.2}$$

When this condition holds, then the form drag and lift are of higher order and can be neglected. Relation (7.2) can be somewhat simplified by using (6.2) and the application of (5.3) to Amazonian eddies (i.e., Ro = 1/2) which gives,

$$\frac{3(2g'\hat{h}_1)^{1/2}}{\beta R_{d\ell}^2 \sin\alpha} \ll 1, \tag{7.3}$$

where $R_{d\ell}$ is the deformation radius of the lower layer $(g'H)^{1/2}/f_0$.

We see that the condition is satisfied when $\hat{h}_1 \to 0$; it is, therefore, expected that thin eddies will obey (7.3). For Amazonian eddies the left-hand side of (7.3) is O(0.1), showing that our neglect of form drag and lift is certainly adequate. However, it should be stressed that, as already pointed out, many eddies at midlatitude (such as Gulf Stream rings) do not satisfy (7.3); therefore, the model is limited to a very specific kind of eddies.

The second assumption which should be verified is the smallness of the perturbations. This assumption is satisfied as long as the critical longshore current speed is small compared to the swirl speed. Using (6.2) and (5.1) with Ro = 1/2 we find that the condition is met when,

$$\frac{\beta(2g'\hat{h}_1)^{1/2} \sin\alpha}{3f_0K} \ll 1. \tag{7.4}$$

We see that this assumption is also satisfied when $\hat{h}_1 \to 0$, showing that it is consistent with our previous assumption regarding the neglect of form drag. For the numerical values given by (6.1) and the value of K discussed earlier (2×10^{-6} s^{-1}), the left-hand side of (7.4) is O(0.1) indicating that the neglected terms are small so that the assumption is adequate. It should be pointed out that both (7.3) and (7.4) are not very sensitive to the numerical values given by (6.1). If slightly different values had been chosen, similar values for the left-hand side of (7.3) and (7.4) would have been obtained.

Although we have demonstrated, using scaling arguments, that our assumptions are valid, we have not really proven the correctness of our solution. This is because in order to prove that our solution is correct, one needs to solve the full first-order problem (i.e., $u^{(1)}$, $v^{(1)}$, $\psi^{(1)}$). The first-order solutions in problems like this usually give compatibility conditions which must be satisfied and may be more restrictive than (7.3) and (7.4). Scaling arguments may, therefore, be insufficient for showing the correctness of our solution; this is probably the most serious weakness of the proposed model. This is also true for the open ocean eddies described in Nof (1981b, 1982 and 1983b) for which the first-order solutions were not originally found either.

It is now known that the model described in Nof (1981b, 1982) is not subject to any first-order limitations because Killworth (1983) and Flierl (1984) have recently found the complete first-order solution and showed that the compatibility conditions do not introduce any additional constraints. This suggests that an attempt to find the complete first-order solution for the problem at hand should also be made. However, the open ocean lens described in Nof (1981b, 1982) is considerably simpler than the present problem and it is not at all clear that the most general first-order solution (for the problem in question) can ever be found analytically. It is, therefore, left as a subject for further investigation.

Before concluding our present discussion it is appropriate to comment on the relationship between the recent studies of Flierl *et al.* (1983), Flierl (1984) and our present investigation. These recent studies examined the general properties of isolated eddies in a frictionless two-layer ocean on a β-plane. They found that an eddy which is truly isolated in both layers (i.e., its velocity decays away from the center) should satisfy general constraints associated with conservation of angular momentum. Specifically, they argue that the total angular momentum should vanish if the eddy is, indeed, isolated in both layers.

It is not clear that these results can be applied to our present model because of the presence of the wall and the possibility that the actual flow under the eddy is not completely isolated, in the sense that it may contain a wake so that the disturbances in the lower layer may not decay away from the eddy. In view of these considerations, it is impossible to tell, without performing a detailed analysis, whether or not the flow under the eddy should compensate for the angular momentum of the eddy. However, even if it does compensate, then the associated motions are

$$O\left(f_0 \frac{\hat{h}_1}{H} \ell_1\right) \sim 1 \text{ cm s}^{-1}.$$

Namely, they are much smaller than the critical lower layer speed and do not enter the first-order problem.

8. Summary

Apart from demonstrating that thin lenslike eddies adjacent to boundaries behave in a different way than their open-ocean counterparts, our model gives important information regarding their interaction with longshore currents. As any other analytical model, our model is applicable to a limited range of parameters and circumstances. In particular, our results are limited to 1) eddies whose densities can be taken to be uniform in space and time, 2) eddies whose internal friction is negligible and 3) eddies whose central depth is very small compared to the depth of the current in which they are embedded. Scaling arguments suggest that Amazonian eddies satisfy these conditions but it should be kept in mind that not all eddies will follow the behavior predicted by our model. The results of the study can be summarized as follows:

i) A thin lenslike eddy situated near a western boundary can remain stationary if it is embedded in a frictional northward flowing current whose speed depends on β and the characteristics of the eddy. This conclusion is valid for both linear and nonlinear eddies and results from the fact that the eddy's net β-induced force (which is directed southward) is balanced by a northward pressure gradient which is directly transmitted from the current to the eddy.

ii) A lenslike eddy situated near an eastern boundary can never remain stationary regardless of the characteristics of the boundary current since as the longshore flow passes, it exerts two forces on the eddy. One counteracts the eddy's β-induced force [as mentioned in i)] and the other acts in a cross-stream direction. The latter pushes the eddy toward the wall in the western boundary case and toward the open ocean in the eastern boundary case.

iii) The speed of the longshore current (flowing from low to high latitudes) that is required to keep the eddy in a fixed position near a western boundary is approximately

$$V \approx \beta R_d^2 \sin\alpha/3\left(\frac{K}{f_0}\right)(1 - \mathrm{Ro}),$$

where R_d is the eddy's deformation radius, Ro the Rossby number, α the inclination of the coast (measured clockwise from the western direction), f_0 the Coriolis parameter and K the frictional coefficient for the longshore current.

iv) It is expected that a current stronger than that given in iii) will carry the eddy *downstream* (i.e., from low to high latitudes), whereas a weaker current will let the eddy drift *upstream* (from high to low latitudes).

Application of (i), (iii), and (iv) to Amazonian eddies suggests that these eddies are carried to the eastern Caribbean by the Guiana Current which has a speed ($\sim$1 m s^{-1}) considerably higher than that required to keep the eddies stationary ($\sim$20 cm s^{-1}). It is also suggested that the observed flattening of the eddy edge near the coast (Fig. 7) results from the presence of β and the Guiana Current which press the eddy against the wall.

Acknowledgments. I thank R. Mied for useful comments regarding an earlier version of this paper. This study was supported by the Office of Naval Research Grants N000-14-75-C-0201 and N000-14-82-C-0404.

REFERENCES

Borstad, G. A., 1982a: The influence of the meandering Guiana Current and Amazon River discharge on surface salinity near Barbados. *J. Mar. Res.*, **40**, 421–434.

——, 1982b: The influence of the meandering Guiana Current on surface conditions near Barbados—temporal variations of Trichodesmium (Cyanophyta) and other plankton. *J. Mar. Res.*, **40**, 435–452.

Csanady, G. T., 1979: The birth and death of a warm core ring. *J. Geophys. Res.*, **84**, 777–780.

Flierl, G. R., 1977: The application of linear quasi-geostrophic dynamics to Gulf Stream rings. *J. Phys. Oceanogr.*, **7**, 365–379.

——, 1984: Rossby wave radiation from a strongly nonlinear warm eddy. *J. Phys. Oceanogr.*, **14**, 47–58.

——, M. E. Stern and J. Whitehead, 1983: The physical significance of modons: Laboratory experiments and general integral constraints. *Dyn. Atmos. Oceans*, **7**, 233–263.

Gibbs, R. J., 1970: Circulation in the Amazon River estuary and adjacent Atlantic Ocean. *J. Mar. Res.*, **38**, 113–132.

Gorshkov, S. G., 1978: *World Ocean Atlas*, Vol. 2, *Atlantic and Indian Oceans*, Pergamon Press, 306 pp.

Killworth, P. D., 1983: On the motion of isolated lenses on a beta-plane. *J. Phys. Oceanogr.*, **13**, 368–376.

Lai, D. Y., and P. L. Richardson, 1977: Distribution and movement of Gulf Stream rings. *J. Phys. Oceanogr.*, **7**, 670–683.

Landis, R. C., 1971: Early BOMEX results of sea surface salinity and Amazon River water. *J. Phys. Oceanogr.*, **1**, 278–281.

Nof, D., 1981a: On the dynamics of equatorial outflows with application to the Amazon's basin. *J. Mar. Res.*, **39**, 1–29.

——, 1981b: On the β-induced movement of isolated baroclinic eddies. *J. Phys. Oceanogr.*, **11**, 1662–1672.

——, 1982: On the movements of deep mesoscale eddies in the North Atlantic. *J. Mar. Res.*, **40**, 57–74.

——, 1983a: The translation of isolated cold eddies on a sloping bottom. *Deep-Sea Res.*, **39**, 171–182.

——, 1983b: On the migration of isolated eddies with application to Gulf Stream rings. *J. Mar. Res.*, **41**, 399–425.

Ring Group, 1981: Gulf Stream cold-core rings: Their physics, chemistry, and biology. *Science*, **212**, 1091–1100.

Rooth, C., 1972: A linearized bottom friction law for large-scale oceanic motions. *J. Phys. Oceanogr.*, **2**, 509–510.

Ryther, J. H., D. W. Menzel and N. Corwin, 1967: Influence of the Amazon River outflow on the ecology of the western tropical Atlantic I. Hydrography and Nutrient Chemistry. *J. Mar. Res.*, **25**, 69–83.

Shen, C. Y., 1981: On the dynamics of a solitary vortex. *Dyn. Atmos. Oceans*, **5**, 239–267.

Stommel, H. M., 1948: The westward intensification of wind-driven ocean currents. *Trans. Amer. Geophys. Union*, **29**, 202–206.

Veronis, G., 1966: Wind driven ocean circulation. Part I. Linear theory and perturbation analysis. *Deep-Sea Res.*, **13**, 17–31.

——, 1981: Dynamics of large-scale ocean circulation. *Evolution of Physical Oceanography*, B. Warren and C. Wunsch, Eds., The MIT Press, 623 pp.

Warren, B. A., 1967: Notes on translatory movement of rings of current with application to Gulf Stream eddies. *Deep-Sea Res.*, **14**, 505–524.